JOURNAL OF VIROLOGY, Mar. 2003, p. 3247–3256 Vol. 77, No. 5
0022-538X/03/$08.00+0 DOI: 10.1128/JVI.77.5.3247–3256.2003

Effects of Point Mutations in the Major Capsid Protein of Beet Western Yellows Virus on Capsid Formation, Virus Accumulation, and Aphid Transmission

V. Brault,[1] M. Bergdoll,[2] J. Mutterer,[2] V. Prasad,[2]† S. Pfeffer,[2] M. Erdinger,[1] K. E. Richards,[2] and V. Ziegler-Graff[2]*

UR-BIVV, INRA, Colmar 68021 Cedex,[1] and Institut de Biologie Moléculaire des Plantes du CNRS et de l'Université Louis Pasteur, Strasbourg 67084 Cedex,[2] France

Received 15 October 2002/Accepted 5 December 2002

Point mutations were introduced into the major capsid protein (P3) of cloned infectious cDNA of the polerovirus beet western yellows virus (BWYV) by manipulation of cloned infectious cDNA. Seven mutations targeted sites on the S domain predicted to lie on the capsid surface. An eighth mutation eliminated two arginine residues in the R domain, which is thought to extend into the capsid interior. The effects of the mutations on virus capsid formation, virus accumulation in protoplasts and plants, and aphid transmission were tested. All of the mutants replicated in protoplasts. The S-domain mutant W166R failed to protect viral RNA from RNase attack, suggesting that this particular mutation interfered with stable capsid formation. The R-domain mutant R7A/R8A protected ~90% of the viral RNA strand from RNase, suggesting that lower positive-charge density in the mutant capsid interior interfered with stable packaging of the complete strand into virions. Neither of these mutants systemically infected plants. The six remaining mutants properly packaged viral RNA and could invade *Nicotiana clevelandii* systemically following agroinfection. Mutant Q121E/N122D was poorly transmitted by aphids, implicating one or both targeted residues in virus-vector interactions. Successful transmission of mutant D172N was accompanied either by reversion to the wild type or by appearance of a second-site mutation, N137D. This finding indicates that D172 is also important for transmission but that the D172N transmission defect can be compensated for by a "reverse" substitution at another site. The results have been used to evaluate possible structural models for the BWYV capsid.

Beet western yellows virus (BWYV; genus *Polerovirus*), like all members of the family *Luteoviridae*, is transmitted in a circulative, nonpropagative manner by aphids (see reference 7 for a review). Poleroviruses and luteoviruses (the other major genus of the family) are transmitted vector specifically, implying that determinants on the viral capsid selectively interact with specific structures within vector aphids. The particles of polero- and luteoviruses are composed of two types of protein, the major capsid protein (P3) of 22 to 23 kDa and a minor species of ~75 kDa known as readthrough (RT) protein (see reference 13 for a review). The RT protein is a C-terminally extended form of P3 produced by episodic suppression of P3 translation termination so that translation continues into the downstream open reading frame (ORF) 5, which encodes the RT domain (12). The RT protein is believed to be incorporated into the capsid via its P3 moiety, with the RT domain protruding from the virion surface (1, 4).

Nicotiana clevelandii can be agroinfected with full-length BWYV cDNA (10), and the resulting plants can serve as a virus source in aphid transmission experiments (1). Site-directed mutagenesis of the viral cDNA prior to agroinfection has been used to map sequences in the RT domain important for virus movement in planta and for aphid transmission of BWYV (1–3). In this paper, we describe the results of a similar search for functionally important determinants located on P3. Eight nonsynonymous point mutations were introduced into BWYV P3, mainly at sites predicted to lie on the capsid surface. The mutations were then tested for their impacts on viral capsid formation, accumulation of the virus in protoplasts and in planta, and aphid transmission. Two mutations interfered with packaging of full-length viral RNA into stable virions. The encapsidation-defective mutants multiplied in protoplasts but did not systemically infect whole plants. The six remaining P3 mutants multiplied on plants, and five were transmitted by aphids with moderate to high efficiency. For one of these mutants, successful transmission events were accompanied either by reversion to the wild-type sequence or by a second-site mutation at a P3 residue which was 45 residues upstream of the primary mutation site in P3. The findings are discussed in the light of possible structural models for the BWYV capsid.

MATERIALS AND METHODS

Construction of mutants of BWYV. All point mutants were created by primer extension mutagenesis (9) using pBW_0 DNA as a template and the oligonucleotides BW22 (nucleotides [nt] 3314 to 3331 of BWYV RNA [22]) and BW23 (complementary to nt 4139 to 4156) as external primers. Partially overlapping plus- and minus-sense mutagenic primers containing the desired amino acid substitutions were designed essentially as described previously (9). The primer sequences are available upon request.

The resulting PCR fragments were cleaved with *Afl*II (which cuts after nt 3339) and *Acc*I (which cuts after nt 4093) and cloned into a pKS (Stratagene)

* Corresponding author. Mailing address: Institut de Biologie Moléculaire des Plantes du CNRS et de l'Université Louis Pasteur, 12 rue du General Zimmer, Strasbourg 67084 Cedex, France. Phone: (33) 388417263. Fax: (33) 388614442. E-mail: veronique.ziegler-graff@ibmp-ulp.u-strasbg.fr.

† Present address: Unit of Phytovirology, Department of Botany, Lucknow University, Lucknow, India.

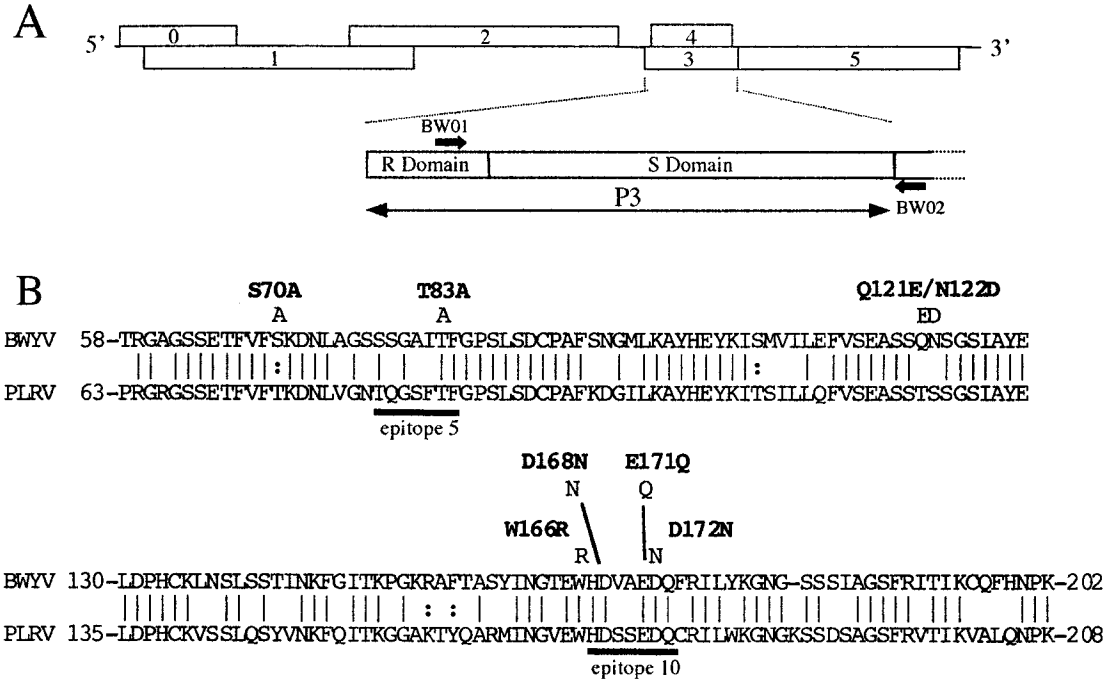

FIG. 1. (A) Genetic organization of BWYV RNA. Important ORFs are represented by numbered rectangles, and untranslated sequences are represented by horizontal lines. The major coat protein (P3) gene and the P3 R and S domains are shown below. The thick arrows indicate the positions of primers used to analyze progeny virus RNA sequences as described in the text. (B) Alignment of the S-domain sequences of BWYV and PLRV and positions of the BWYV S-domain mutations. The alignment was produced by SEQLAB. The vertical lines indicate identical amino acids, and the semicolons indicate similar amino acids (S and T, R and K, and F and Y). The positions of epitopes 5 and 10 (20) in the PLRV capsid are indicated below the PLRV sequence. The positions of point mutations introduced into the BWYV S domain are shown above the sequences.

derivative containing the same sites. The various cloned inserts were sequenced using a model 373 DNA sequencer (Applied Biosystems) to verify that each contained only the desired alteration. A full-length viral cDNA clone containing each mutation was assembled by first adding an *Acc*I-*Nco*I (nt 4192 to 4822) fragment to the cloned mutagenized *Afl*II-*Acc*I fragment in the pKS derivative vector and then replacing the wild-type *Afl*II-*Nco*I (nt 3339 to 4822) fragment in the transcription vector pBW_0 (23) with the corresponding fragment bearing the mutation. The region bearing the mutation was sequenced again in the full-length cDNA clone to insure that the desired substitution had been achieved.

Mutant BWYV cDNA constructs for agroinfection were made by replacing the wild-type BWYV cDNA sequence in the binary plasmid $pBinBW_0$ (1) with a restriction fragment containing the mutation to produce the plasmids pBinS70A, pBinT83A, etc. The substitution was carried out by replacing the *Spe*I-*Sal*I fragment (extending from nt 1350 to a polylinker site 32 nt downstream of the insert 3′ terminus) of $pBinBW_0$ with the *Spe*I-*Sal*I fragment from the corresponding mutant transcription vector. The resulting plasmids were introduced into *Agrobacterium tumefaciens* strain LBA4404 for agroinfection.

Infection of protoplasts and plants and aphid transmission assays. Full-length BWYV RNA transcripts were obtained by bacteriophage T7 RNA polymerase transcription of *Sal*I-linearized wild-type or mutated versions of pBW_0 and were inoculated into *Chenopodium quinoa* (3). *N.clevelandii* plants were agroinfected (1) with *A. tumefaciens* LBA4404 harboring a binary expression vector containing wild-type or mutant BWYV cDNA sequences. Infected plants were identified 4 to 5 weeks postinoculation by double-antibody sandwich (DAS)–enzyme-linked immunosorbent assay (ELISA) with a rabbit polyclonal antiserum raised against the virus (3). Virus was purified from upper leaves of agroinfected plants as described previously (21), and experiments with aphid transmission to *Montia perfoliata* used either purified virus or detached leaves from agroinfected plants as the inoculum source (3).

Detection of viral RNA and capsid proteins. Total and RNase-resistant RNAs were extracted from protoplasts as described previously (15). Viral RNA was detected by Northern blotting using a ^{32}P-labeled or digoxigenin-UTP-labeled RNA (Roche Diagnostics) probe complementary to the 3′-terminal 196 nt of BWYV RNA (15). Total RNA from plant tissue was extracted using either Trizol (Invitrogen) or a commercial RNA purification kit (Rneasy Plant Mini-Kit; Qiagen). Viral structural proteins in total-protein extracts of infected protoplasts were detected by Western blotting using antisera specific for the BWYV P3 and RT proteins (2).

Analysis of progeny viral RNA. The stability of the mutations in progeny viral RNA following agroinfection or aphid transmission experiments was examined by amplifying a DNA fragment spanning the mutation site by reverse transcription-PCR (1). Reverse transcription was primed using an oligonucleotide complementary to BWYV nt 4091 to 4107 (BW02), and a PCR fragment was synthesized with oligonucleotides BW01 (nt 3563 to 3578) and BW02 (Fig. 1A). The PCR product was cleaved with *Hin*dIII and *Eco*RI (nonviral sites built into the primers) and cloned into pKS (Stratagene). Insert sequences were determined for randomly selected clones.

Model building. The coordinates of the structural model for the *Potato leafroll virus* (PLRV; genus *Polerovirus*) shell (S) domain were supplied by L. Terradot. The PLRV and BWYV S-domain sequences were aligned with SEQLAB (Accelrys), and the published PLRV structure (19) was used as a template to generate an analogous "Terradot" model for BWYV with MODELLER (17). The alternative model presented in this paper was based on a three-dimensional structure-based sequence alignment of the S domains of seven viral capsid proteins with crystallographically determined structures collected in the HOMSTRAD database (14). The viruses included in the collection were *Tomato bushy stunt virus*, *Southern bean mosaic virus* (SBMV), *Sesbania mosaic virus*, *Satellite panicum mosaic virus*, *Bean-pod mottle virus*, *Cowpea chlorotic mottle virus*, and *Satellite tobacco necrosis virus* type 1. The BWYV capsid sequence was aligned with this structure-based consensus alignment using CLUSTAL X (8). When compared pairwise to the S-domain sequence of each of the seven members of the group, the resulting aligned BWYV S-domain sequence displayed the closest homology with that of SBMV (8% identity and 31% similarity). Minor refinements to the SBMV-BWYV alignment were made using SEQLAB, and the SBMV S-domain crystal structure (18) was then employed as a template to deduce a three-dimensional structure for the BWYV S domain with MODELLER. Manual adjustments of the model were then performed to optimize conservation of the basic jellyroll structure and to eliminate conflicts when the monomer structure was used to generate the asymmetric trimer.

RESULTS AND DISCUSSION

Mutations in the BWYV major capsid protein (P3). No crystallographically determined structure is available for the capsid of any member of the family *Luteoviridae*, but crystallographic studies of other small icosahedral plus-strand RNA viruses have revealed that many of them are constructed according to a common design (reviewed in reference 16). In such virions, the capsid protein can be divided into several domains: (i) the N-terminal R domain, which extends into the capsid interior and has a crystallographically disordered structure; (ii) the central S domain, which forms the bulk of the protective capsid structure; and, in some cases, (iii) an outwardly projecting (P) C-terminal domain. The S domain itself is organized into the so-called jellyroll structure, which is composed of a succession of eight alternately antiparallel β-sheets (known as β-sheets B to I) connected by spacers consisting of extended chains and/or α-helixes. Computer-assisted secondary-structure predictions indicate that the P3s of all luteo- and poleroviruses are of this type (5, 13, 19).

Two short sequences (epitopes 5 and 10 [Fig. 1B]), which are strongly immunogenic and hence presumably exposed on the surface of the capsid, have been mapped on the S domain of PLRV (20). As the amino acid sequences of the S domains of BWYV and PLRV are 68% identical, the two sequences can be readily aligned (Fig. 1B), and we assume that the BWYV sequences corresponding to PLRV epitopes 5 and 10 in the resulting alignment will also be surface located on BWYV. Accordingly, the sequences in the BWYV S domain which corresponded to PLRV epitopes 5 and 10 were chosen as primary targets for point mutation by replacement of chosen residues with nonsynonymous amino acids. In the epitope 5 counterpart sequence of BWYV, T83 (which aligns with a T in epitope 5 of PLRV) was replaced by A to produce the mutant T83A (Fig. 1B). Four point mutations were introduced in or near the epitope 10 counterpart sequence of BWYV (residues 167 to 173 [Fig. 1B]) to produce the mutants W166R, D168N, E171Q, and D172N. In addition to these epitope 5 and 10 mutants, mutant S70A, which targets a serine that is strictly conserved in the S domains of all *Luteoviridae*, and a double mutant (Q121E/N122D), targeting a pair of bulky S-domain residues, were also produced (Fig. 1B). Note that none of the aforesaid mutations in the P3 ORF alters the amino acid sequence of P4, the protein encoded by the overlapping ORF 4. (Fig. 1A).

The N-terminal R domains of the different luteo- and poleroviruses display less sequence similarity than the S domains, but all are characterized by a high content of arginine residues, 37% in the case of the ~48-residue R domain of BWYV. As mentioned above, the R domain is believed to extend into the capsid interior, where the basic residues could interact with the packaged RNA. An R-domain mutant was produced in which a pair of adjacent Rs near the P3 N terminus were replaced by alanines (mutant R7A/R8A). Residues 7 to 8 map upstream of the region where ORFs 3 and 4 overlap, so the substitutions do not alter the P4 sequence.

Effect of the P3 mutations on viral RNA packaging. Full-length BWYV RNA transcripts containing the different P3 mutations were used to infect *C. quinoa* protoplasts. The protoplasts were harvested 48 h postinoculation, and total RNA and proteins were extracted. Northern hybridization of the total RNA using a riboprobe complementary to the 3′-terminal region of the viral RNA revealed that the mutant transcripts were replication competent and produced progeny genomic and subgenomic RNAs in the protoplasts (Fig. 2A). The yields of the genomic and subgenomic RNAs for the mutants were comparable to that obtained for infection with the wild-type viral RNA transcript BW_0, except for mutant W166R, for which yields were reduced by ~80% (Fig. 2A, lane 11). In the transcript-infected protoplasts, the mutants directed synthesis of wild-type or near-wild-type levels of P3 and RT proteins, except for W166R, for which significantly lower levels of both proteins (particularly RT protein) were observed (Fig. 2C, lane

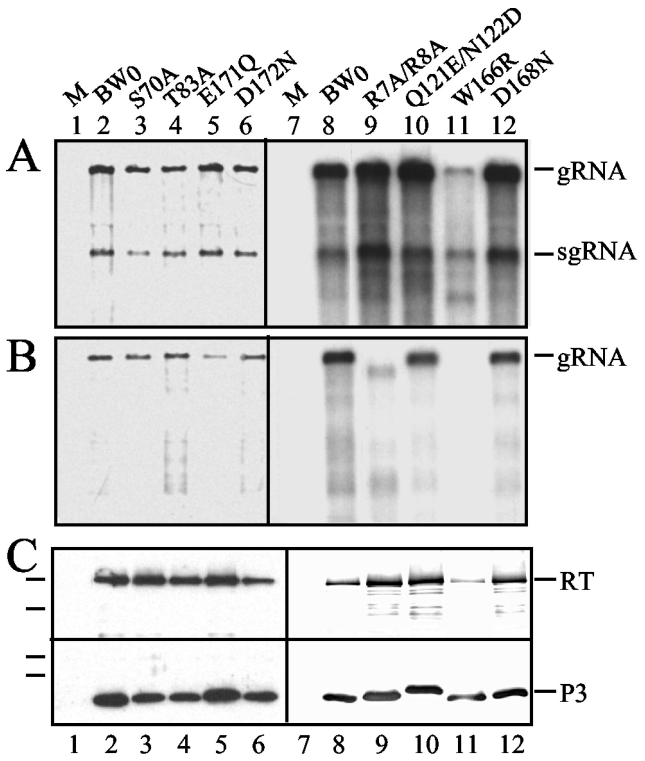

FIG. 2. Amplification in protoplasts of BWYV RNA carrying mutations in the P3 cistron. (A) Northern blot analysis of total RNA extracted from 200,000 protoplasts inoculated with transcripts of BW_0 (lanes 2 and 8), S70A (lane 3), T83A (lane 4), E171Q (lane 5), D172N (lane 6), R7A/R8A (lane 9), Q121E/N122D (lane 10), W166R (lane 11), and D168N (lane 12). RNA extracted from mock-inoculated protoplasts was loaded in lanes 1 and 7. The positions of genomic (g) and subgenomic (sg) RNAs are indicated on the right. (B) Detection of encapsidated viral RNA from infected protoplasts. Total RNA was extracted under conditions in which only virion-packaged RNA remains intact. The lane numbering is as in panel A. In panels A and B, the blots on the left were hybridized with a digoxigenin-labeled riboprobe complementary to the 3′-terminal 196 residues of BWYV RNA. In the blots on the right, the same riboprobe was ^{32}P labeled. (C) Immunodetection of BWYV P3 and RT proteins in protein extracts from protoplasts infected with the above-mentioned mutants. The upper part of the blot was probed with an RT domain-specific antiserum (15), and the lower part was probed with a P3-specific antiserum. The lines on the left indicate the positions of 82-, 49-, 33.5-, and 28.5-kDa molecular-mass markers. Minor species detected by the RT domain-specific antiserum in the upper blot are assumed to be RT protein degradation products.

11). For unknown reasons, P3 of mutant Q121E/N122D migrated more slowly during sodium dodecyl sulfate-polyacrylamide gel electrophoresis than did wild-type P3 and the P3s of the other mutants (compare Fig. 2C, bottom, lane 10 to the other lanes).

A previously described RNase sensitivity assay was used to determine if any of the P3 mutations interfered with packaging of viral RNA into virions. Protoplasts infected with BW_0 and the various P3 mutant transcripts were gently disrupted 48 h postinoculation, and the crude extract was incubated at 37°C for 30 min under conditions in which nonencapsidated BWYV RNA is completely degraded (15). The extract was then subjected to phenol extraction, and protected viral RNA was detected by Northern hybridization as described above. For all of the mutants except W166R, significant amounts of the progeny genomic RNAs in the protoplast extracts were resistant to degradation by this treatment (Fig. 2B). We conclude that, among the S-domain mutants tested here, only the R-for-W substitution in W166R strongly interfered with packaging of the viral RNA into an RNase-resistant form. Based on the available data, we cannot determine if the W166R mutation abolishes virion formation per se or interferes with the stability of the resulting virions to RNase treatment. Whichever explanation proves to be correct, the packaging defect in W166R is presumably responsible, at least in part, for the lower yield of progeny viral RNA in the protoplast infection experiments with this mutant.

Viral RNA in protoplast extracts infected with the R-domain mutant R7A/R8A was packaged in RNase-resistant form at levels ranging in different experiments from 20 to 50% of that observed in a BW_0-infected extract treated in parallel (Fig. 2B, lanes 8 and 9). Interestingly, the protected viral RNA was reproducibly ~400 nt shorter than encapsidated wild-type genomic RNA (Fig. 2B, compare lanes 8 and 9), indicating that ~10% of the RNA strand is not incorporated into the virion or, if taken up, is not packaged in an RNase-resistant form. In preliminary experiments, two additional mutants (R13G/R14G and R43G/R47G) containing a pair of G-for-R substitutions at downstream sites in the R domain similarly failed to encapsidate the entire viral RNA (data not shown). Thus, the packaging defect in R7A/R8A is not related to the particular position of the positively charged residues in the R domain that were targeted for mutagenesis. We suggest that the incomplete packaging observed for these mutants is related to the overall lower positive-charge density of the R domain in the capsid interior (two fewer arginine residues per subunit, corresponding to 360 fewer positive charges in a complete T = 3 capsid). This could diminish the ability of the capsid to accommodate the entire length of the genomic RNA in a form resistant to RNase attack. Note that at least some of the truncated RNA must have been trimmed at the 5′ terminus, since the radioactive probe used in the Northern blot was complementary to the 3′-terminal portion of the viral RNA.

Effects of the P3 mutants upon virus accumulation in agroinfected *N. clevelandii*. The P3 gene sequence containing each of the different point mutations was substituted for the wild-type P3 sequence in $pBinBW_0$ for agroinfection of young *N. clevelandii* plants (1). The virus titer in noninoculated upper leaves of the plants was determined by DAS-ELISA about 4 weeks postinoculation. Virus accumulation levels in the plants agroinfected with the mutants S70A, T83A, Q121E/N122D, D168N, and E171Q were similar to or only moderately lower than the virus levels observed in plants agroinfected with the wild-type construct $pBinBW_0$ (Table 1). Much lower accumulation levels were observed for D172N, and no progeny virus at all was detected in the upper leaves of plants agroinoculated with W166R and R7A/R8A (Table 1). The inability of the mutants with an encapsidation defect (i.e., W166R and R7A/R8A) to invade upper leaves is consistent with earlier observations, demonstrating that virion formation is essential for virus movement in *N. clevelandii* (24).

TABLE 1. Accumulation of BWYV P3 mutants in agroinoculated plants[a]

Mutant	Mean absorbance in plants[b]			
	Expt 1	Expt 2	Expt 3	Expt 4
R7A/R8A		0.01 ± 0.01		
S70A	0.90 ± 0.10		1.30 ± 0.14	
T83A	0.61 ± 0.14		0.94 ± 0.18	
Q121E/N122D		0.51 ± 0.11	1.36 ± 0.25	
W166R		0.00 ± 0.01		
D168N		0.42 ± 0.12	0.83 ± 0.25	
E171Q	0.85 ± 0.11		1.15 ± 0.14	
D172N	0.16 ± 0.03		0.18 ± 0.06	
N137D/D172N				0.40 ± 0.13
BW_0	0.80 ± 0.09	0.77 ± 0.06	1.73 ± 0.15	0.75 ± 0.13

[a] Plant extracts were tested for BWYV by DAS-ELISA about 4 weeks after agroinfection with the indicated construct.

[b] Mean absorbance ± standard error at 405 nm after 1 h of substrate incubation. The background absorbance observed with healthy plant extract (typically 0.11 to 0.12) has been substracted. Each independent experiment was performed with 10 to 23 plants per construct.

Sequences of progeny virus in agroinfected plants. Viruses with an RNA genome are typically subject to a relatively high rate of mutation during replication (6). To investigate the fates of the various P3 mutations during virus amplification in planta, total RNA was extracted from infected upper leaves of plants agroinfected with wild-type $pBinBW_0$ and each of the movement-competent P3 mutants. The sequence corresponding to viral nt 3563 to 4092, which encompasses all but the 5′-terminal 80 nt of the P3 ORF, was amplified by reverse transcription followed by PCR. The resulting DNA fragments were cloned, and the inserts of 4 to 15 randomly selected clones, generally obtained from two or more independent reverse transcription-PCRs, were sequenced.

For two plants agroinfected with $pBinBW_0$, sequence analysis of 13 cloned reverse transcription-PCR fragments detected a total of two nucleotide changes in the region analyzed, neither of which altered the P3 amino acid sequence (Fig. 3A). Such variation in the wild-type progeny sequences was observed earlier in a study of mutants in the BWYV RT domain (2) and is presumably due to a combination of natural sequence "drift" during the relatively error-prone viral RNA multiplication process and errors introduced during reverse transcription-PCR amplification of the sequence to be analyzed.

For S70A, T83A, Q121E/N122D, D168N, and E171Q, the primary mutations were strictly conserved in all the progeny reverse transcription-PCR clones analyzed, but there were occasional nucleotide substitutions elsewhere in the P3 sequence,

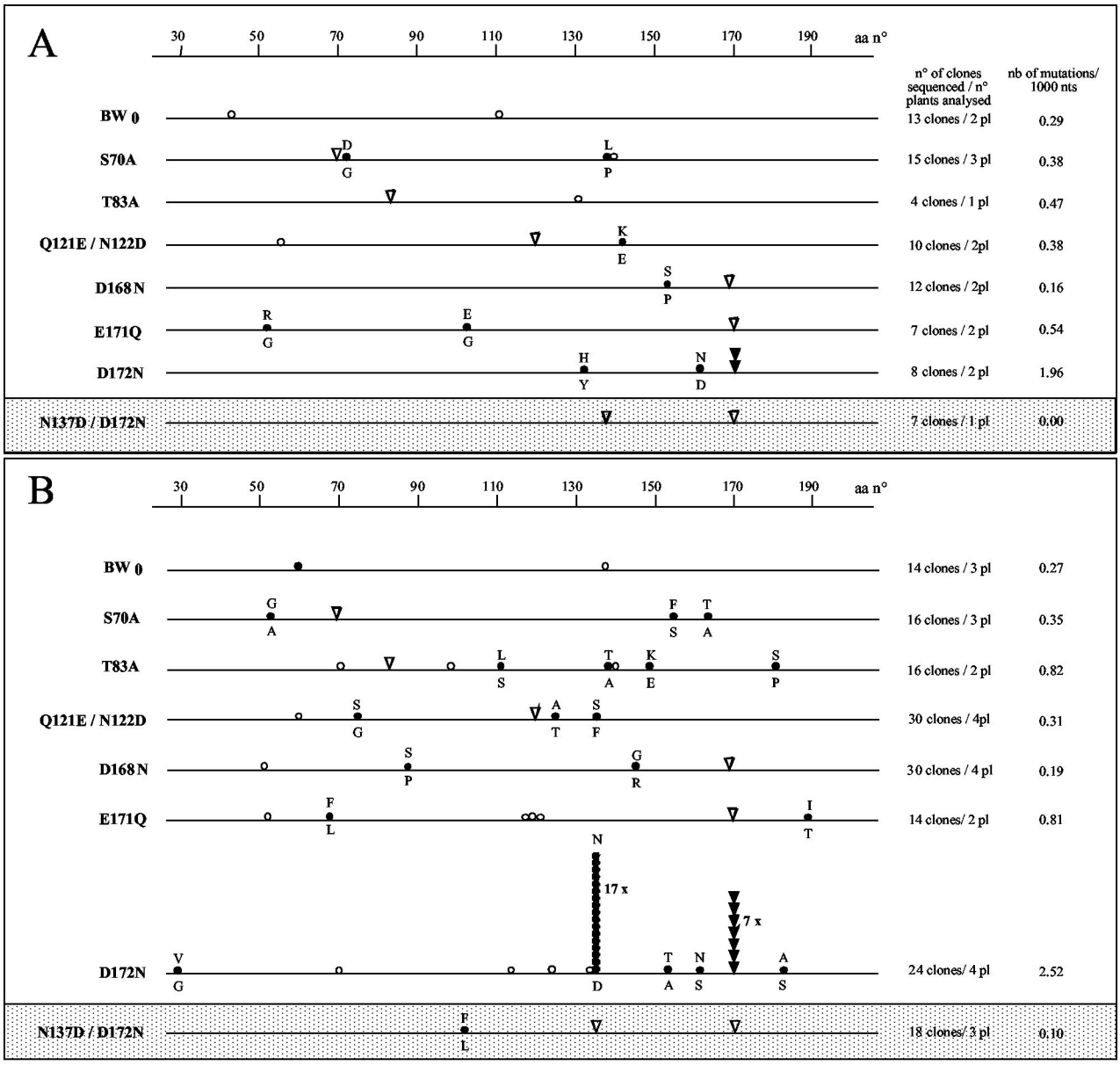

FIG. 3. Distributions of nucleotide mutations detected in viral progeny RNA following agroinfection of *N. clevelandii* with wild-type or mutant BWYV cDNA constructs (A) or after successful aphid transmission of virus from agroinfected leaves or purified virus solutions to *M. perfoliata* (B). The results obtained with the two different types of inoculum did not differ significantly and have been combined. For each construct, the column to the immediate right indicates the total number of reverse transcription-PCR clones sequenced and the number of plants (pl) that were analyzed. The column on the far right indicates the number of nucleotide substitutions observed per 1,000 nt sequenced in the progeny. The position of the primary mutation in each mutant clone is indicated by a triangle. An open triangle indicates that the primary mutation was conserved in the progeny, and a solid triangle indicates that the primary mutation had undergone reversion to the wild-type sequence (observed only for some D172N progeny). The circles symbolize the different second-site nucleotide mutations which were detected in the progeny reverse transcription-PCR clones; an open circle represents a silent mutation, and a solid circle represents a mutation which resulted in an amino acid change in P3 (the wild-type amino acid at each such position is shown above the line, and the observed amino acid substitution is shown below). Stacks of symbols indicate that the mutation in question was detected multiple times. The ladder at the top of each panel refers to the amino acid (aa) position in P3.

some of which provoked changes in the P3 amino acid sequence (Fig. 3A). The overall rate at which the nucleotide substitutions occurred in the mutant progeny, however, was fairly similar to that observed for the background variation in the BW_0 progeny, i.e., 0.16 to 0.54 substitutions per 1,000 nt sequenced in the different mutant progeny versus 0.29/1,000 nt sequenced for the wild-type progeny. Furthermore, there was no obvious pattern to the natures or positions of the observed P3 amino acid substitutions in the mutant progeny (Fig. 3A), suggesting that none of them represents a specific second-site mutation which has been selected for because it counteracts a hypothetical lack of fitness of the primary mutant for prolifer-

TABLE 2. Aphid transmission of BWYV P3 mutants

Mutant	Transmission[a]			
	Agroinfected *N. clevelandii*		Purified virus	
	8[b]	30	8	30
S70A	18/18	15/15		
T83A	6/6	5/6		
Q121E/N122D	1/16	3/11	0/8	1/17
D168N	5/15	7/9	3/8	4/6
E171Q	0/6	3/5	3/8	3/4
D172N	3/6	4/9	8/8	9/9
BW_0	16/16	9/9	16/16	16/16
N137D/D172N	11/17	12/12		
BW_0	14/14	6/6		

[a] The virus sources were (i) *N. clevelandii* leaves 4 to 5 weeks after agroinoculation with the indicated mutant and (ii) virus purified from plants agroinfected with the indicated mutant. Purified virus was diluted to 25 μg/ml for BW_0 and for all mutants except Q121E/N122D, which was diluted to 50 μg/ml. The results of transmission are presented as the number of plants infected after aphid transmission (determined by DAS-ELISA)/number of plants tested.

[b] Number of aphids per plant.

ation in *N. clevelandii*. Finally, it should be mentioned that some of the scattered nucleotide substitutions which appeared in the progeny sequences following agroinfection altered the amino acid sequence of P4. It has been shown elsewhere, however, that P4 is dispensable for systemic infection of *N. clevelandii* (24), so it is highly unlikely that the P4 mutations have a significant effect on virus accumulation levels.

In the case of mutant D172N, four point mutations were observed in the eight progeny reverse transcription-PCR clones characterized, and all four mutations altered the P3 amino acid sequence (Fig. 3A). Two of the substitutions presumably correspond to background mutations in the P3 sequence (H133Y and N162D), but the two others were identical and resulted in reversion of the mutated residue, N172, to the wild-type D. Although the number of progeny clones analyzed is insufficient to draw strong conclusions, this finding suggests that the D172N mutant may be less effective than the wild type for proliferation in *N. clevelandii* so that selective pressure favors enrichment in the progeny virus population of a variant which has regained the wild-type sequence. It appears likely, however, that the D172N mutant is at least partially functional, since it still persisted as a major component of the population 4 weeks postinfection.

Aphid transmission of virus from agroinfected plants. To evaluate the effect of the P3 mutations on virus-vector interactions, either *N. clevelandii* agroinfected with the P3 mutants or virus purified from such plants was used as an inoculum in aphid transmission experiments. Nonviruliferous *M. persicae* nymphs were allowed a 24-h aquisition access period on upper leaves of the agroinfected plants or on a solution of purified virus prior to transfer to *M. perfoliata* test plants for a 4-day inoculation access period. The test plants were then assayed for virus infection 3 to 4 weeks later by DAS-ELISA. The two sources of inoculum (agroinfected leaves and purified virus) gave similar results in the transmission assays (Table 2). Of the six mutants that were tested, all were aphid transmitted with moderate to high efficiency, except for mutant Q121E/N122D, which was poorly transmitted from both agroinfected leaves (4 of 27 test plants infected) and purified virus solution (1 of 25 test plants infected) (Table 2).

Sequence analysis of progeny virus in aphid-inoculated plants. To determine if successful transmission of the P3 mutants is accompanied by reversion to the wild-type sequence or the appearance of specific compensatory second-site mutations, total RNA was extracted from the infected target plants, and the sequence corresponding to the P3 gene was amplified by reverse transcription-PCR, cloned, and sequenced as described above. As a control, analysis of 14 reverse transcription-PCR clones from plants that had been aphid infected with virus from plants agroinfected with $pBinBW_0$ revealed two nucleotide substitutions (one of which altered the P3 amino acid sequence [Fig. 3B]), for a frequency of 0.27 substitutions per 1,000 nt sequenced. As mentioned above, we assume that these alterations result from occasional misreading of the template sequence by the viral RNA replicase during virus multiplication in planta and/or during reverse transcription-PCR amplification.

For S70A, T83A, Q121E/N122D, D168N, and E171Q, the primary mutations were strictly conserved in all of the sequenced progeny reverse transcription-PCR clones following aphid transmission. Although the observed frequency of substitution for T83A and E171Q (~0.8/1,000 nt sequenced) was somewhat higher than for the wild-type and the other mutant progeny, there was no clustering of the resulting P3 amino acid substitutions at any particular sites in any of the above-mentioned mutants (Fig. 3B), as would be expected if there was strong selection in the aphid-transmitted progeny virus population for compensatory second-site mutations.

A different situation prevailed for mutant D172N. Analysis of 24 reverse transcription-PCR clones from four separate plants revealed that successful aphid transmission was invariably accompanied either by reversion of the primary mutation to the wild type (observed in seven clones, all obtained from RNA from the same plant) or by a second-site substitution in which N137 was replaced by a D (observed in the remaining 17 reverse transcription-PCR products obtained from all four plants) (Fig. 3B). The second-site mutation did not alter the P4 amino acid sequence. Finally, in addition to the reversion of the primary mutation and the N137D second-site mutation observed in all the aphid-transmitted D172N progeny, eight other substitutions (four affecting the P3 amino acid sequence) were dispersed along the sequenced portion of the P3 gene (Fig. 3B). Since these sequence variants do not cluster, we assume that they correspond to background misreading during viral replication and/or reverse transcription-PCR.

Properties of an N137D/D172N double mutant. The absence of virus carrying only the D172N mutation from the progeny following aphid transmission indicates that D172 is an important determinant in this process. The appearance of the second-site mutation N137D in all the aphid-transmitted progeny which conserved the primary D172N mutation represents strong circumstantial evidence that the N137D substitution can compensate for the putative transmission defect associated with the primary mutation. To test this hypothesis directly, a double mutant containing both substitutions was constructed and used to agroinfect *N. clevelandii*. The mutant (N137D/D172N) accumulated to somewhat lower levels than BW_0 (Table 1, experiment 4) but was readily transmitted from the

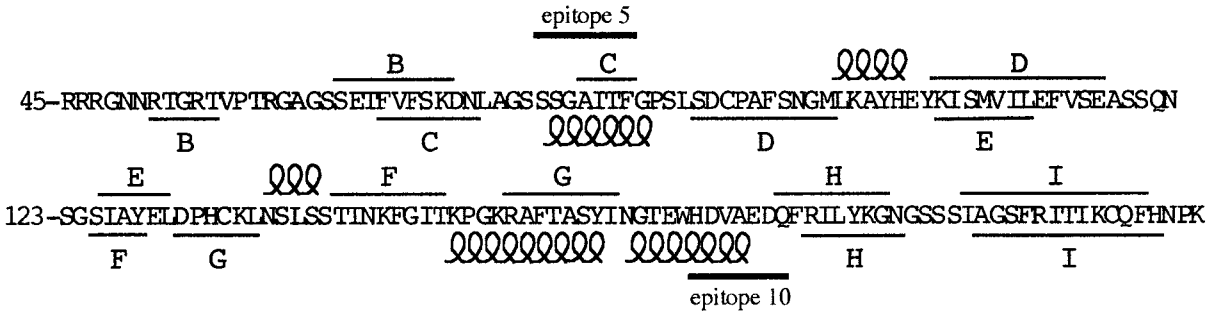

FIG. 4. BWYV P3 S-domain residues predicted to be in β-sheets (horizontal lines) and α-helices (loops) in the Terradot model (symbols above the sequence) and in the alternative model proposed in this paper (symbols below the sequence). The positions of the BWYV counterparts of PLRV epitopes 5 and 10 are indicated by thick lines.

agroinfected leaves to test plants (Table 2). Analysis of cloned viral cDNA following reverse transcription-PCR as described above revealed that neither the N137D nor the D172N substitution underwent alteration in either the agroinoculated plants (Fig. 3A) or the aphid-infected plants (Fig. 3B), and no hot spot for other second-site mutations was observed.

Mapping the P3 mutations on a model for the BWYV capsid. As noted above, computer-assisted secondary-structure predictions indicate that the S domains of the luteo- and polerovirus capsids conform to the β-sheet jellyroll structure characteristic of the capsids of a number of other small icosahedral plant viruses (5, 13, 19). A model for the capsid structure of PLRV has recently been proposed based upon an alignment of the PLRV S domain with the known crystal structure of the S domain of *Rice yellow mottle virus* (genus *Sobemovirus*), with which it shows 17% identity and 33% sequence similarity (19). The resulting model, which we refer to as the Terradot model, is consistent with the immunological data in that epitopes 5 and 10 are situated on the outer surface of the capsid (19).

Since the S domains of all poleroviruses display extensive sequence identity, the PLRV structure can be used as a template to produce very similar capsid models for the other members of the family, including BWYV (19). Figure 4 shows the positions along the BWYV S-domain sequence of β-sheets and α-helices predicted from the PLRV-BWYV alignment. Figure 5A shows the three-dimensional structure of the BWYV S domain of an A subunit based on the Terradot model, where A refers to the conformation of a subunit at a 5′-fold axis of symmetry of a complete virion. (B and C refer to the closely similar conformations of subunits at a pseudosixfold axis of symmetry.) In a computer-generated asymmetric unit composed of an A, a B, and a C subunit, W166 (a residue which is conserved in all poleroviruses) is situated near the trimer center, where it could interact with residues in neighboring subunits to stabilize the capsid (19). This localization is evidently consistent with our observation that the mutation W166R interferes with stable virion formation.

For poleroviruses, the Terradot model predicts the existence of a "patch" of conserved acidic residues near the center of the capsid trimer, and it was suggested that this feature may be important for molecular recognition of virions at different stages of the virus infection cycle (19). In the Terradot model for BWYV, the acidic-patch residues correspond to E104, E165, D168, E171, and D172. As noted above, our findings show that D172 is indeed implicated in virus-aphid interactions. In contrast, our mutations targeting two other putative acidic-patch residues (D168N and E171Q) did not abolish virus accumulation in planta or aphid transmission, although the levels observed were somewhat lower than in the wild type (Tables 1 and 2). Whether or not the acidic patch does in fact exist on the BWYV capsid in the conformation predicted by the Terradot model (see below), it is evident that residues D168, E171, and D172 will be in close proximity in any structural model. Thus, the fact that, in contrast to D172N, the D168N and E171Q mutants can still be transmitted by aphids (albeit less efficiently than the wild type) indicates that the presence of a particular number of negative charges in the vicinity of D172 is not in itself an absolute requirement for transmissibility.

Of particular interest in testing a capsid model are those mutations which strongly interfere with aphid transmission (i.e., Q121E/N122D and D172N), as the residues targeted in these mutants are expected to lie on the capsid surface. In the Terradot model, Q121 and N122 are situated in the loop connecting β-sheets D and E and fall on the outer surface of the structure (Fig. 5A), consistent with a role in virus-aphid interactions. It should be noted, however, that Q121 and N122 map to a vertex of the subunit and hence will be juxtaposed at the 20 pseudosixfold and 12 fivefold axes of the complete T = 3 virion. The Terradot structure thus requires that the Q121E/N122D double mutant accommodate 10 or 12 extra negative charges at each of these sites without interfering with stable capsid formation, a requirement which, in our opinion, casts some doubt upon whether the residues in question are properly mapped in the Terradot model.

The results with D172N provide another opportunity to test the Terradot structure. We have shown above that successful transmission of this mutant is accompanied either by reversion to the wild-type sequence or by the appearance in the progeny of a reverse second-site mutation, N137D. One possible interpretation of this finding is that the charge density on the capsid surface is important for virus-aphid interactions and that the viral variant with the second-site mutation is selected for because it restores the wild-type surface charge density. This situation has been observed for a mutation introduced into the coat protein of *Cucumber mosaic virus* (11). In the context of our findings with P3, however, a similar hypothesis does not readily explain why the mutations D168N and E171Q, which

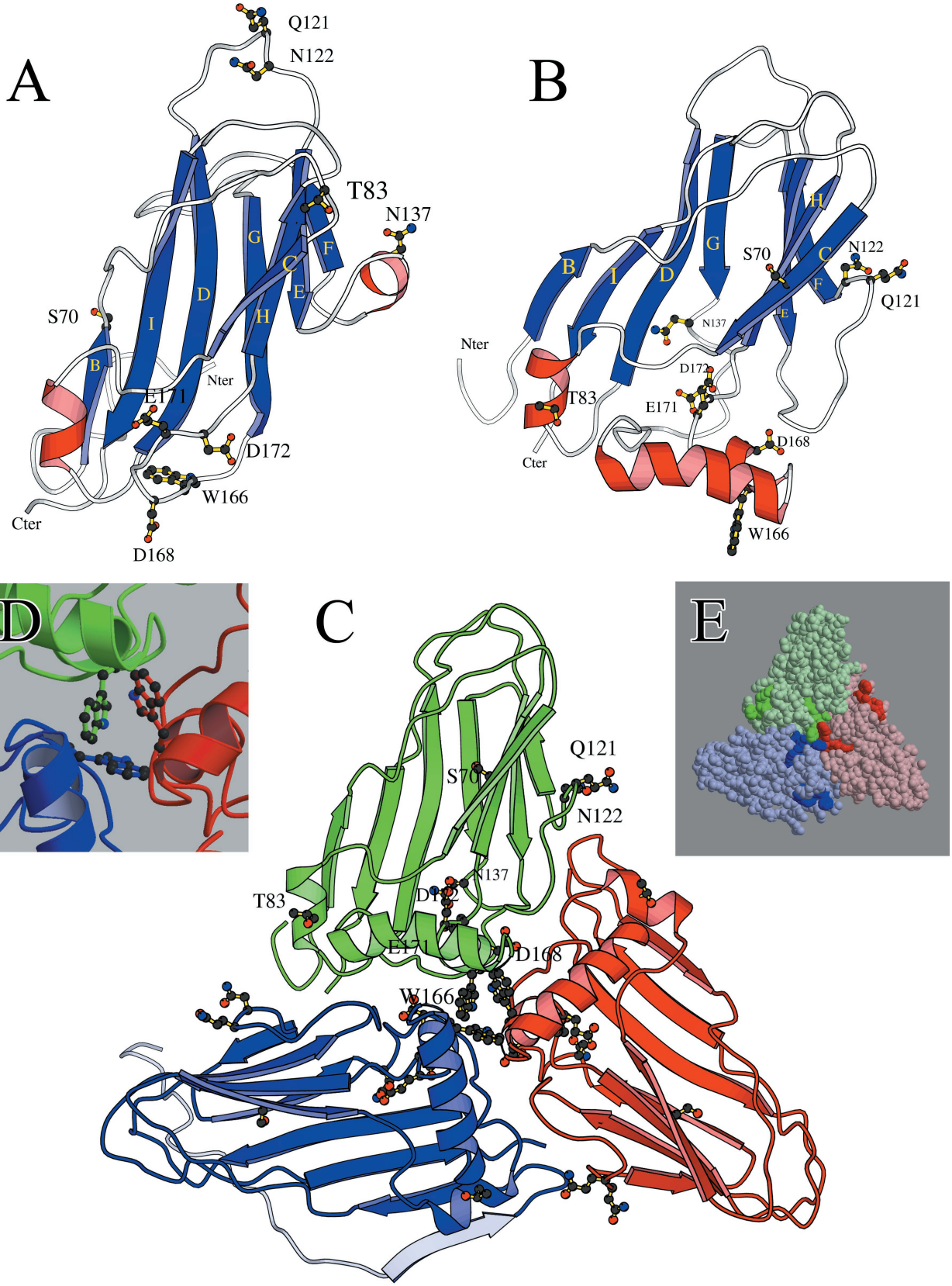

FIG. 5. (A and B) Structures of the BWYV S domain (A conformation) predicted in the Terradot model (19) (A) and in this paper (B). The views look down on the outer surface, and amino acid residues targeted for mutation in the present work are identified. The blue ribbons correspond to β-sheets, and the red coils correspond to α-helices (Fig. 4). The R domain, which is believed to extend into the capsid interior from the N terminus of the S domain (Nter), is not shown. (C) Asymmetric trimer of subunits in the A (green), B (red), and C (blue) conformations derived from our BWYV P3 S-domain structure (panel B). Amino acids targeted for mutation are identified in the green subunit. For the blue subunit, the R domain is shown in light blue. The β-sheet (light blue ribbon) near the C terminus of the R domain was predicted by computer modeling (unpublished observations), but the rest of the R domain sequence is depicted as an arbitrarily drawn disordered structure. (D) Positions of W166 residues on the subunits at the center of the trimer shown in panel C. Chains in different subunits are colored as in panel C. (E) Solid-surface representation of the structure shown in panel C. The darker colors on each subunit indicate the positions of residues corresponding to PLRV epitope 5 (the elongated structures near the sides of the triangle) and epitope 10 (the trilobate structures at the center).

target residues near D172 and which would also be expected to alter the surface charge density, remain functional in transmission.

An alternative explanation for the transmissibility of D172N/N137D is that a noncovalent interaction important for aphid transmission occurs between D172 and N137 in the wild-type capsid. The N137D second-site mutation could reestablish the capacity of capsid protein carrying the D172N primary mutation to form this bond. Such a hypothesis, however, requires that N137 be located near D172, a condition not fulfilled in the Terradot model, where N137 is in an α-helix in the loop joining β-sheets E and F and is separated from D172 by 2.4 nm (Fig. 5A).

An alternative structural model for the BWYV S domain. In light of the difficulty of the Terradot model in accounting for certain of our findings, it is interesting to consider an alternative structural model for the BWYV capsid. The structure was derived independently of the Terradot model by aligning the BWYV S-domain sequence with an S-domain consensus alignment for seven viruses of the β-sheet jellyroll family for which crystallographic structures are available (see Materials and Methods). An important and unexpected difference between our alignment and that used to produce the Terradot model is that the positions of the first six β-sheets (i.e., β-sheets B to G) are shifted toward the N terminus on the P3 sequence relative to the Terradot assignments (Fig. 4). However, the presence of a long connecting loop between β-sheets G and H in our model brings β-sheets H and I back into near register with their counterparts in the Terradot model (Fig. 4).

Our sequence alignment between the BWYV S domain and the other viral S domains was then used to generate a three-dimensional structure for the BWYV S domain, using the SBMV S-domain crystal structure (18) as a template. In the resulting BWYV structure (Fig. 5B), most of the residues corresponding to PLRV epitopes 5 and 10 are surface accessible (Fig. 5E). The sequence corresponding to the PLRV epitope 5 motif is mainly situated on a predicted surface α-helix in the loop connecting β-sheets C and D (Fig. 5B and E) and will lie near A-B and C-C subunit contacts between neighboring asymmetric units in the complete virion (data not shown). The sequence 167-HDVAEDQ-173, corresponding to PLRV epitope 10, is mostly located on an α-helix which forms one side of a shallow depression on the capsid surface near the center of the capsid trimer (Fig. 5E). The portion of the epitope including residues 171-EDQ-173 extends into the depression itself (Fig. 5B).

Our alternative structure resembles the Terradot model in that W166 lies near the center of the asymmetric unit (Fig. 5C and D). Thus, as in the Terradot model, the inability of mutant W166R to form stable virions could be related to charge repulsion interference with intersubunit contacts in this region. Q121 and N122 in our model are situated in the loop joining β-sheets E and F (Fig. 5B) and are surface accessible, consistent with the observation that mutation of these residues interferes with aphid transmission. Contrary to the Terradot model, however, Q121 and N122 are not situated on the subunit at positions where they will be juxtaposed with their counterparts on neighboring subunits in the full capsid structure (data not shown), which is more readily reconciled with our finding that the extra charged residues in mutant Q121E/N122D do not interfere with stable capsid formation. Finally, in our model, residue D172 is situated in a shallow depression on the capsid surface (Fig. 5B), which could be a recognition site in virus-aphid interactions. Importantly, our model locates N137 near D172, so the two residues could potentially interact (Fig. 5B).

Concluding remarks. Until crystallographic data are available, model building based on homology with viruses of other families is the only available means of gaining insight into luteovirus capsid structure. Such an approach is rendered difficult in the case of the *Luteoviridae* by the fact that their capsid proteins display only low sequence similarity with the capsids of structurally characterized viruses which can serve as templates. It is thus to be expected that any luteovirus capsid structure derived by model building will require constant reevaluation as new experimental data emerge. The D172N/N137D covariation associated with successful aphid transmission reported here is one such finding: it is not readily explained by the Terradot model, whereas our alternative model can potentially account for it by bringing the two residues into close proximity in three dimensions. Another interesting point is that the residues identified here as important for aphid transmission (D172 and Q121/N122) do not map near one another in either of the available structural models. We cannot rule out the possibility that, for example, the Q121E/N122D mutation acts at a distance to provoke subtle structural changes near D172 which are in fact responsible for the transmission defect. Alternatively, the BWYV particle could possess two or more discrete "vector interaction subdomains." Such subdomains could function at different steps in the acquisition-transmission process, a hypothesis which is amenable to experimental test. Future research will be aimed at further testing the available luteovirus capsid models with additional BWYV P3 mutants and the use of chemical probes to investigate residue accessibility on virions.

ACKNOWLEDGMENTS

We thank Laurent Terradot for providing the coordinates of his PLRV S-domain structure.

V.P. benefited from a grant from the Ministère des Affaires Etrangères.

REFERENCES

1. **Brault, V., J. F. J. M. van den Heuvel, M. Verbeek, V. Ziegler-Graff, A. Reutenauer, E. Herrbach, J. C. Garaud, H. Guilley, K. Richards, and G. Jonard.** 1995. Aphid transmission of beet western yellows luteovirus requires the minor capsid readthrough protein P74. EMBO J. **14:**650–659.
2. **Brault, V., J. Mutterer, D. Scheidecker, M. T. Simonis, E. Herrbach, K. Richards, and V. Ziegler-Graff.** 2000. Effects of point mutations in the readthrough domain of beet western yellows virus minor capsid protein on virus accumulation in planta and on transmission by aphids. J. Virol. **74:**1140–1148.
3. **Bruyère, A., V. Brault, V. Ziegler-Graff, M. T. Simonis, J. F. J. M. van den Heuvel, K. Richards, H. Guilley, G. Jonard, and E. Herrbach.** 1997. Effects of mutations in the beet western yellows virus readthrough protein on its expression and packaging, and on virus accumulation, symptoms and aphid transmission. Virology **230:**323–334.
4. **Cheng, S. L., L. L. Domier, and C. J. D'Arcy.** 1994. Detection of the readthrough protein of barley yellow dwarf virus. Virology **202:**1003–1006.
5. **Dolja, V. V., and E. V. Koonin.** 1991. Phylogeny of capsid proteins of small icosahedral RNA plant viruses. J. Gen. Virol. **72:**1481–1486.
6. **Domingo, E., and J. J. Holland.** 1997. RNA virus mutations and fitness for survival. Annu. Rev. Microbiol. **51:**151–178.
7. **Gildow, F. E.** 1999. Luteovirus transmission and mechanisms regulating vector specificity, p. 88–113. *In* H. G. Smith and H. Barker (ed.), The luteoviruses. CAB International, Wallingford, United Kingdom.
8. **Higgins, D., J. Thompson, T. Gibson, J. D. Thompson, D. G. Higgins, and**

T. J. Gibson. 1994. CLUSTAL W: improving the sensitivity of progressive multiple sequence alignment through sequence weighting, position-specific gap penalties and weight matrix choice. Nucleic Acids Res. **22:**4673–4680.

9. **Ho, S. N., H. D. Hunt, R. M. Horton, J. K. Pullen, and L. Pease.** 1989. Site-directed mutagenesis by overlap extension using the polymerase chain reaction. Gene **77:**51–59.
10. **Leiser, R. M., V. Ziegler-Graff, A. Reutenauer, E. Herrbach, O. Lemaire, H. Guilley, K. Richards, and G. Jonard.** 1992. Agroinfection as an alternative to insects for infecting plants with beet western yellows luteovirus. Proc. Natl. Acad. Sci. USA **89:**9136–9140.
11. **Liu, S., X. He, G. Park, C. Josefsson, and K. L. Perry.** 2002. A conserved capsid protein surface domain of cucumber mosaic virus is essential for efficient aphid vector transmission. J. Virol. **76:**9756–9762.
12. **Mayo, M. A., and W. A. Miller.** 1999. The structure and expression of luteovirus genomes, p. 23–42. *In* H. G. Smith and H. Barker (ed.), The luteoviruses. CAB International, Wallingford, United Kingdom.
13. **Mayo, M. A., and V. Ziegler-Graff.** 1996. Molecular biology of luteoviruses. Adv. Virus Res. **46:**413–460.
14. **Mizuguchi, K., C. M. Deane, T. L. Blundell, and J. P. Overington.** 1998. HOMSTRAD: a database of protein structure alignments for homologous families. Protein Sci. **7:**2469–2471.
15. **Reutenauer, A., V. Ziegler-Graff, H. Lot, D. Scheidecker, H. Guilley, K. Richards, and G. Jonard.** 1993. Identification of beet western yellows luteovirus genes implicated in viral replication and particle morphogenesis. Virology **195:**692–699.
16. **Rossmann, M. G., and J. E. Johnson.** 1989. Icosahedral RNA virus structure. Annu. Rev. Biochem. **58:**533–573.
17. **Sali, A., and T. L. Blundell.** 1993. Comparative protein modelling by satisfaction of spatial restraints. J. Mol. Biol. **234:**779–815.
18. **Silva, A. M., and M. G. Rossmann.** 1987. Refined structure of southern bean mosaic virus at 2.9 Å resolution. J. Mol. Biol. **197:**69–87.
19. **Terradot, L., M. Souchet, V. Tran, and D. Giblot Ducray-Bourdin.** 2001. Analysis of a three-dimensional structure of potato leafroll virus coat protein obtained by homology modeling. Virology **286:**72–82.
20. **Torrance, L.** 1992. Analysis of epitopes on potato leafroll virus capsid protein. Virology **191:**485–489.
21. **van den Heuvel, J. F. J. M., T. M. Boerma, and D. Peters.** 1991. Transmission of potato leafroll virus from plants and artificial diets by *Myzus persicae*. Phytopathology **81:**150–154.
22. **Veidt, I., H. Lot, R. M. Leiser, V. Ziegler-Graff, H. Guilley, K. Richards, and G. Jonard.** 1988. Nucleotide sequence of beet western yellows virus RNA. Nucleic Acids Res. **16:**9917–9932.
23. **Veidt, I., S. E. Bouzoubaa, R. M. Leiser, V. Ziegler-Graff, H. Guilley, K. Richards, and G. Jonard.** 1992. Synthesis of full-length transcripts of beet western yellows virus RNA: messenger properties and biological activity in protoplasts. Virology **186:**192–200.
24. **Ziegler-Graff, V., V. Brault, J. Mutterer, M. T. Simonis, E. Herrbach, H. Guilley, K. E. Richards, and G. Jonard.** 1996. The coat protein of beet western yellows luteovirus is essential for systemic infection but the viral gene products P29 and P19 are dispensable for systemic infection and aphid transmission. Mol. Plant-Microbe Interact. **9:**501–510.